Reproductive Toxicology 136 (2025) 108973

Contents lists available at ScienceDirect

Reproductive Toxicology

journal homepage: www.elsevier.com/locate/reprotox

Impact of particulate matter 2.5 on placental ultrastructure including mitochondrial damage through oxidative stress

Gain Lee [a], Jung Mi Han [c], Young-Ah You [b], Yoon-Young Go [b], Sunwha Park [b], Young Min Hur [b], Soo Min Kim [a], Ki-Hwan Han [d], Young Ju Kim [a,b,*]

[a] Graduate Program in System Health Science and Engineering, Ewha Womans University, Republic of Korea
[b] Department of Obstetrics and Gynecology and Ewha Medical Institute, College of Medicine, Ewha Womans University, Republic of Korea
[c] Nano Imaging Laboratory in the Ewha Medical Research Institute, Ewha Womans University, Republic of Korea
[d] Department of Anatomy, College of Medicine, Ewha Womans University, Republic of Korea

ARTICLE INFO

Handling Editor: Dr. Bal-Price Anna

Keywords:
Particulate matter 2.5
Placenta
Syncytiotrophoblast
Transmission electron microscopy
Oxidative stress
Mitochondrial damage

ABSTRACT

Introduction: Particulate matter 2.5 ($PM_{2.5}$) refers to fine particles with a diameter of less than 2.5μm, associated with adverse pregnancy outcomes. The study aims to determine whether elevated prenatal $PM_{2.5}$ levels were associated with alterations in the ultrastructure of the placenta and mitochondria, potentially linked to oxidative stress.

Methods: The placental samples were collected from the Air Pollution on Pregnancy Outcome (APPO) cohort and were classified into two groups based on $PM_{2.5}$ exposure levels: the High group (> 15 μg/m^3; n = 9) and the Low group (≤ 15 μg/m^3; n = 8). Transmission electron microscopy was used to assess the ultrastructure of the placenta, specifically the syncytiotrophoblast area. The structure of the mitochondria in the fetal capillaries was also analyzed. Malondialdehyde (MDA) and superoxide dismutase 2 (SOD2) were quantified by using enzyme-linked immunosorbent assays (ELISA).

Results: The High group placenta showed ultrastructural changes including microvilli loss, basement membrane thickening, vacuolation and swollen endoplasmic reticulum (ER). Microvilli were significantly shortened and lost in the High group ($P < 0.005$). Swollen vacuoles, ER stress, and basement membrane thickening were observed in High group syncytiotrophoblast ($P < 0.005$). Mitochondria in fetal capillaries from the High group were also damaged, showing disrupted double membranes and cristae ($P < 0.05$). MDA and SOD2 levels were significantly upregulated in the High group ($P < 0.05$).

Conclusion: Prenatal exposure to $PM_{2.5}$ may be associated with alterations of placental ultrastructure and mitochondrial damage in fetal capillaries, potentially mediated by oxidative stress, as indicated by elevated levels of MDA and SOD2.

1. Introduction

Particulate matter 2.5 ($PM_{2.5}$) refers to particles with a diameter smaller than 2.5μm. Due to their small size, they can enter the bloodstream and circulate through the terminal alveoli via respiratory movements [1]. Exposure to air pollution is associated with a burden of adverse health effects [2]. The harmful effects of long–and short–term exposure to $PM_{2.5}$ have been well-documented [3]. Especially, prenatal exposure to air pollution is associated with adverse pregnancy outcomes including preterm birth (PTB), gestational diabetes mellitus (GDM), small gestational age (SGA), and intrauterine growth restriction (IUGR) [4].

Although the mechanism by which $PM_{2.5}$ leads to adverse health outcomes has not been fully elucidated, reactive oxygen species (ROS)

Abbreviations: APPO, Air Pollution on Pregnancy Outcome; BMI, Body mass index; EDS, Energy-dispersive X-ray spectroscopy; ELISA, Enzyme-linked immunosorbent assay; ER, Endoplasmic reticulum; GDM, Gestational diabetes mellitus; HCG, Human Chorionic gonadotrophin; IUGR, Intrauterine growth restriction; LTE, Long-term evolution; MDA, Malondialdehyde; MMP, Mitochondrial membrane potential; NICU, Neonatal intensive care unit; OXPHOS, Oxidative phosphorylation; PlGF, Placental growth factor; $PM_{2.5}$, Particulate matter 2.5; PTB, Preterm birth; ROS, Reactive oxygen species; SGA, Small gestational age; SOD2, Superoxide dismutase 2; TEM, Transmission electron microscopy.

* Correspondence to: Anyangcheon-ro, Yangcheon-gu, Seoul 07985, Republic of Korea.
E-mail address: kkyj@ewha.ac.kr (Y.J. Kim).

https://doi.org/10.1016/j.reprotox.2025.108973
Received 26 March 2025; Received in revised form 4 June 2025; Accepted 9 June 2025
Available online 10 June 2025
0890-6238/© 2025 The Authors. Published by Elsevier Inc. This is an open access article under the CC BY license (http://creativecommons.org/licenses/by/4.0/).

generation has been suggested as the key mechanism that causes systemic inflammation [5] and also may directly affect the fetus [6]. Mitochondria, which generate cellular energy through oxidative phosphorylation, have a dynamic structure that responds to damage from free radicals and influences their cellular fate [7]. Excessive exposure to $PM_{2.5}$ leads to mitochondrial dysfunction, accompanied by increased ROS [8] and apoptosis of macrophage foam cells via loss of mitochondrial membrane potential (MMP) [9]. Our previous research revealed that mitochondrial oxidative phosphorylation (OXPHOS) dysfunction was significantly higher in cord blood exposed to high levels of $PM_{2.5}$ [10].

The placenta is a temporally and structurally complex organ that facilitates the exchange of nutrients, waste, and oxygen between the mother and fetus [11]. The central role of the placenta is not only to mediate these exchanges but also to protect the fetus from the vertical transmission of pathogens [12]. The syncytiotrophoblast establishes a barrier between the mother and fetus and directly contacts the maternal blood [11]. Additionally, the syncytiotrophoblast produces hormones and growth factors such as human chorionic gonadotropin (hCG), progesterone, estrogens, placental growth factor (PlGF), and soluble fms-like tyrosine kinase-1 to maintain a healthy pregnancy [13].

Placental morphological adaptations in response to pathology are associated with structural alterations in structure such as loss of microvilli [14]. Maternal or fetal disorders, including chorioamnionitis, villitis, maternal hypertension syndrome, and stillbirth, are significantly associated with amniotic epithelial basement membrane thickening [15]. Additionally, cytoplasmic vacuolation and endoplasmic reticulum (ER) swelling are observed in the placentae exposed to hypoxic conditions [16]. These aberrant placental pathologies may be induced by SGA, impaired maternal angiogenesis, and exposure to particulate matter [17–19]. While the effects of increased concentration of $PM_{2.5}$ on testicular spermatogenic tubules, sperm quality, and testosterone biosynthesis are well documented, its impact on placental structure and organelles remains less understood [20]. The study of the pathological ultrastructure of the placenta is important as it reflects the pathophysiology of pregnancy-related complications.

Thus, this study aims to evaluate the morphometric assessment of placental ultrastructural alterations, including changes in mitochondrial structure in the endothelial cells of the fetal capillaries when exposed to high levels of $PM_{2.5}$ using transmission electron microscopy (TEM). Additionally, the expression of the oxidative stress marker lipid malondialdehyde (MDA) and antioxidants superoxide dismutase 2 (SOD2) in the placental tissue was measured to reveal the related mechanism of ROS induction by high level of $PM_{2.5}$.

2. Method

2.1. Study population

This was a nested case-control cohort study based on a prospective cohort Air Pollution on Pregnancy Outcome (APPO) study. The APPO study recruited more than 1200 participants from January 2021 to December 2023 at seven university hospitals. We previously reported the details of the APPO cohort study [21]. This study was approved by the Ethical Research Committees of the centers (Ewha Womans University Mokdong Hospital, EUMC 2021–04–032) and conducted according to the ethical principles of the Helsinki Declaration. All the participants provided written informed consent.

Pregnancy outcomes including gestational age at delivery, delivery mode, infant sex, birth weight, birth height, Apgar score, and neonatal intensive care unit (NICU) admission were recorded. All singleton pregnant women were recruited at Ewha Womans University Mokdong Hospital for sample normalization and precision. Nine participants were included in both the control and exposure groups; however, one participant from the control group was excluded because of the failure to collect individual $PM_{2.5}$.

2.2. $PM_{2.5}$ exposure assessment

Daily outdoor $PM_{2.5}$ concentrations were collected from a nearby urban atmospheric measurement network based on the residential addresses of the study subjects. The Urban Air Monitoring Station data used in this study were obtained from Air Korea (https://www.airkorea.or.kr/web) of The Korean Ministry of the Environment.

The household indoor $PM_{2.5}$ concentrations were measured using the electronic device AirguardK® (Kweather, Co., Seoul, Korea) which can detect indoor air pollution levels with a light-scattering laser photometer sensor. The device was installed in the participants' living room for at least 1 week during each trimester of pregnancy. The device was connected to the internet at one-minute intervals to measure $PM_{2.5}$ in real-time. The measured data were then stored in the indoor air quality monitoring long-term evolution (LTE) communication network to prevent data loss. Participants completed a time-activity questionnaire for one week, providing detailed information regarding their daily activities and locations [4,21,22]. We calculated individual $PM_{2.5}$ exposure using a time-weighted average model that considers the duration and location of various activities, using collected outdoor and indoor $PM_{2.5}$, and the time-activity patterns [23]. The time-weighted model is as follows:

$$C_{estimates} = \{(C_{household} \times T_{household}) + (C_{indoors\ not\ at\ home} \times T_{indoors\ not\ at\ home}) + (T_{outdoor} \times C_{outdoor})\} \div 24\ h$$

$C_{estimates}$: personalized estimates of PM exposure

$C_{household}$: household PM concentration

$T_{household}$: time spent at home

$C_{indoors\ not\ at\ home}$: average of household PM concentration per trimester of pregnancy for all participants

$T_{indoors\ not\ at\ home}$: time spent indoors not at home

$C_{outdoor}$: outdoor PM concentration

$T_{outdoor}$: time spent outdoor

We defined participants who were exposed to $PM_{2.5}$ concentration above 15 μg/m^3 as the High group and below 15 μg/m^3 defined as the Low group according to the World Health Organization's air quality guidelines World Health Organization [24].

2.3. Collection of placenta samples for analysis

Placenta samples were collected immediately following delivery or cesarean section. The placenta was dissected under the chorio-amniotic membrane (~5 cm away from the cord insertion side) where at the fetal side-placenta some area to avoid infarction and hematomas [6]. The fresh placenta was collected under aseptic conditions and cut into 0.5 − × 0.5 − × 0.5 − mm and fixed using 2.5 % glutaraldehyde in 0.1 M phosphate buffer (pH 7.4) for TEM examination. To quantify oxidative stress markers and antioxidant enzymes, placenta samples were stored at − 80 ℃ until analysis.

2.4. TEM analysis

To investigate the ultrastructure of PM-induced placental degeneration, we employed a comprehensive experimental approach. Placental tissue samples were collected from individuals exposed to both low and high $PM_{2.5}$. Subsequently, these samples were subjected to meticulous processing for TEM, enabling the detailed visualization of cellular and subcellular alterations. Following the initial fixation, specimens were washed in 0.1 M phosphate buffer and subsequently fixed with 1 % osmium tetroxide in 0.1 M phosphate buffer (pH 7.4) for 1 h. The samples were dehydrated using ethanol and embedded in epoxy resin. Ultrathin sections, with thickness ranging between 60 and 70 nm were prepared using an ultramicrotome (Leica EMUC7, Vienna, Austria) equipped with a diamond knife. These sections were contrasted with uranyl acetate followed by lead citrate to enhance visualization. Subsequently, we examined the prepared samples using an H-7650 TEM microscope by Hitachi, Tokyo, Japan, operating at an accelerating voltage of 80 kV.

2.5. Morphometric assessment of placenta using TEM

A quantitative examination was performed to assess the degree of the placental damage by observing different grids containing ten random placenta ultrathin section fields for each sample (Table 1). For systemic quantitative analysis, ultrathin sections were examined at 5000 × , 10,000 × , 20,000 × , 50,000 × , and 100,000 × magnification. To reduce potential statistical bias due to the limitation of sample size, tissue selections were randomly collected from the ten different regions and analyzed in a blind manner.

To assess these morphologic alterations, we measured four specific parameters of the placenta: 1) The perpendicular length of microvilli from the intravascular area to the edge of syncytiotrophoblast; 2) syncytiotrophoblast proportion, calculated as the ratio of syncytial tissue area to the total area, excluding regions containing vacuoles and areas of ER swelling; 3) the thickness of syncytiotrophoblast-side basement membrane, measured as perpendicular length; and 4) the ratio of altered mitochondrial structure analyzed in endothelial cells of the fetal capillaries. The open-source image software Image J (National Institutes of Health, Bethesda, MD, USA) was used for the measurements.

2.6. Measurement of oxidative stress marker and mitochondrial antioxidant enzyme

Samples were selected from the APPO cohort, including TEM-analyzed samples. The levels of the oxidative stress marker MDA and the superoxide dismutase enzyme SOD2 were quantified using enzyme-linked immunosorbent assay (ELISA) kits. Frozen placental samples were washed with cold phosphate-buffered saline (PBS) and homogenized at 20 m/s for 20 s using a FastPrep-24 Homogenizer (MP Biomedicals, LLC, USA). To measure the concentrations of MDA and SOD2 in the placentae, a colorimetric lipid peroxidation assay kit (ab118970; Abcam, Cambridge, UK) and a human SOD2 ELISA kit (ab178012; Abcam, Cambridge, UK) were used. Each procedure was performed according to the manufacturer's instructions.

2.7. Statistical analysis

All statistical analyses were performed using SPSS Software (version 19; IBM, Armonk, NY, USA). Continuous variables were analyzed using the independent *t*-test or the Mann–Whitney *U* test, depending on normality. Categorical variables were compared using Fisher's exact test or the chi-square test, as appropriate. Bonferroni correction was applied for multiple comparisons where necessary. Continuous variables are expressed as mean ± standard deviation, and categorical variables are expressed as total number (n) and percentage (%).

Table 1
Scoring criteria for loss of terminal microvilli, mitochondrial abnormalities, and vacuolation in syncytiotrophoblast characteristic.

Assessment Area	Score	Criteria
Microvilli density	−	None (normal)
	+	Shortening or colonization
	+ +	Significant modifications including loss
	+ ++	Almost absence
Mitochondria abnormality	−	None (normal), Double membrane existence
	+	Fission or swelling, loss of double membrane
	+ +	Disrupt of cristae or rupture of outer membrane
	+ ++	Morphological alteration
Swelling of vacuoles and/or endoplasmic reticulum	−	None (normal)
	+	Mild distance, Scarce presence
	+ +	Moderate presence
	+ ++	Distant distension presence. Sporadic ribosome

Quantitative evaluation was performed using 10 random syncytiotrophoblast fields from each sample at 5000 × , 10,000 × , 20,000 × , 50,000 × , and 100,000 × magnifications. Each field was evaluated in a blinded manner.

3. Result

3.1. Characteristics of study subjects

The average $PM_{2.5}$ concentration of the Low group was 9.69 ± 4.01 μg/m^3 and the High group was 27.90 ± 11.68 μg/m^3 ($P < 0.001$). There were no significant differences in clinical characteristics, including maternal age, prenatal body mass index (BMI), white blood cell count, hs-CRP level, prevalence of pregnancy complications, and gestational week at delivery between the two groups. The current and passive smoke states were not significantly different. Neonatal characteristics, including infant sex, weight, 1-min and 5-min Apgar scores, and neonatal intensive care unit (NICU) admission, were also not significantly different (Table 2). To assess potential confounding factors, we conducted a survey evaluating maternal nutritional status, cooking methods, socioeconomic status, delivery method, and overall stress levels. No significant differences were found between the Low and the High groups (data not shown).

3.2. TEM analysis

3.2.1. Comprehensive placenta morphology assessment

Ten randomly selected sections from individual samples were comprehensively assessed according to our criteria (Table 1). The High group placentae showed the presence of a detached microvillus fraction and its shortening. Swelling of the ER and vacuoles, disruption of the mitochondrial double membrane, and altered cristae were predominantly observed in the High group (Supplementary 1). Based on our scoring criteria, features categorized as normal or unaltered were defined as '− (none)', while those scoring from '+ ' to '+ ++ ' were

Table 2
Clinical characteristics of study subject.

Characteristic	Low (n = 8)	High (n = 9)	*P* value
Concentration of $PM_{2.5}$ (μg/m^3)	9.69 ± 4.01	27.90 ± 11.68	< 0.001
Maternal age (years)	33.00 ± 3.74	36.33 ± 4.61	0.125
Pre-pregnancy BMI (kg/m^2)	20.07 ± 2.38	21.13 ± 2.69	0.497
White blood cells (10^3/uL)	7.62 ± 1.56	9.80 ± 2.17	0.143
Gestational week at delivery (weeks)	37.34 ± 2.18	38.52 ± 0.93	0.287
hs-CRP (mg/dL)	1.01 ± 0.70	1.28 ± 1.23	0.596
Adverse pregnancy outcomes, n (%)			
Preterm birth	3 (37.5)	0 (0.0)	0.285
Preeclampsia	1 (12.5)	0 (0.0)	0.471
GDM	1 (12.5)	2 (22.2)	0.424
SGA	1 (12.5)	0 (0.0)	0.471
Current smoking, n(%)	0 (0)	0 (0)	1.000
Passive smoking, n(%)	2 (25.0)	2 (22.2)	0.424
Infant sex, n(%)			0.204
Male	4 (50.0)	2 (22.2)	
Female	4 (50.0)	7 (77.8)	
Birth weight (g)	2805.56 ± 442.24	3106.67 ± 301.04	0.170
NICU administration, n (%)	2 (22.2)	4 (44.4)	0.285
Apgar score 1 min	9.33 ± 1.12	8.22 ± 1.86	0.198
Apgar score 5 min	9.89 ± 0.33	8.22 ± 1.72	0.309

To examine variations in continuous and categorical variables, a Mann-Whitney *U* test, analysis of variance, and Fisher's exact test were applied as necessary. Data are presented as mean and standard deviation (SD) or number and percentage. Abbreviation: BMI, body mass index; GDM, gestational diabetes mellitus; hs-CRP, high sensitivity C-reactive protein; SGA, small gestational age.

grouped as '+ (present)'. The High group had a significantly higher proportion of '+ (present)' cases. (Table 3, $P < 0.001$). Several lysosomal bodies, lipid droplets, and fibrosis were observed in the connective tissue in the High group; however, the differences were not significant (data not shown).

3.2.2. Shortening of microvilli and vacuolation and ER swelling in syncytiotrophoblast tissue

Microvilli, the outermost layers of the syncytiotrophoblast, are in direct contact with the maternal intravascular area. The consistent microvilli and dense placental organ were observed in the Low group (Fig. 1A, B), whereas an irregular form of microvilli was displayed in the High group placenta (Fig. 1D, E). The length of microvilli in the High group placenta (714.71 ± 274.76 nm) was significantly shortened compared to the Low group (1757.98 ± 538.65 nm, $P < 0.001$) (Fig. 1G). Even the loss of microvilli and the absence of zones were observed in the High group.

Additionally, ER swelling and dilated cytosolic vacuoles were observed in the High group syncytiotrophoblast tissue (Fig. 1F). The proportion of tissue sections from syncytiotrophoblast cells without ER swelling and cytosolic vacuoles was significantly greater in the Low group (78.83 ± 13.57 % vs. 58.19 ± 17.09 %, $P < 0.001$) (Fig. 1C).

3.2.3. Basement thickening and unknown nano substances were observed in the high group

The basement membrane is the first barrier of the placenta that protects fetal blood vessels. The basement membrane of the syncytiotrophoblast-side barrier was degenerated and significantly thicker in the High group (3184.56 ± 1653.55 nm) compared to the Low group (688.89 ± 566.25 nm, $P < 0.001$) (Fig. 2). Detachment from syncytiotrophoblast and degradation were also observed in the High group (Supplementary Fig. 1).

Additionally, the ultrathin sections of the High group placenta displayed the presence of unknown nanoparticles. These nanoparticles were observed in the syncytiotrophoblast-side basement membrane (Fig. 3A, D) and within fetal capillaries (Fig. 3B, E). In addition, unidentified encapsulated substances were observed in the epithelial cells of fetal blood vessels (Fig. 3C, F).

3.2.4. Damaged mitochondria structure in fetal capillary

The mitochondria in syncytiotrophoblast have an irregular and smaller architecture [7]. Therefore, alterations in fetal capillary mitochondria in connective tissue were the primary focus of this study. In the Low group placenta, mitochondria have been observed to maintain a double membrane and cristae structure. (Fig. 4A, C). In the case of the mitochondria in the High group (Fig. 4D) showed structural changes, including rupture of the double membrane (Fig. 4E), swelling (Fig. 4F, G), spiral cristae (Fig. 4H), darkening (Fig. 4I), and elongation or fragmentations, potentially reflecting imbalances in mitochondrial dynamics (Fig. 4J). The High group had a significantly greater ratio of damaged mitochondria out of the total number of mitochondria in fetal capillaries (45.04 ± 15.81 %, $P < 0.05$) than in the Low group (29.84 ± 15.53 %, Fig. 4B).

Table 3
Quantitative assessment result by exposed particulate concentration within syncytiotrophoblast tissue.

		Low (n = 80#)	High (n = 90#)	*P* value
Microvilli loss	− (none)	25 (31.25)	9 (11.25)	< 0.001
	+ (Present)	55 (68.75)	81 (88.75)	
Damaged mitochondria	− (none)	22 (27.50)	13 (16.25)	< 0.001
	+ (Present)	58 (72.50)	77 (58.75)	
Swelling of vacuoles and/or endoplasmic reticulum	− (none)	15 (18.75)	1 (1.25)	< 0.001
	+ (Present)	65 (81.25)	89 (98.75)	

Data are presented as numbers and percentages of occurrence. The chi-square test was used to compare the quantitative assessments. According to our criteria, normal or no alteration is grouped into the '− (none)' category scoring from + to + ++ categorized into '+ (present)'. # To reduce individual disparities, ten randomly selected fields of vision were recorded and examined per placenta.

3.3. Oxidative stress marker and the antioxidants enzyme expression

To investigate the oxidative stress in the placenta tissue, 12 placenta samples from the Low group and 13 from the High group were selected from the APPO cohort, including the samples used for TEM analysis. We measured the expression levels of the oxidative stress marker MDA (Fig. 5A) and the antioxidant enzyme SOD2 (Fig. 5B) using an ELISA kit. The concentration of the MDA was significantly higher in the High placentae (6.67 ± 0.82 ng/mg) than in the Low group. The SOD2 levels in the placenta from the High group (19.57 ± 3.72 ng/ml, $P < 0.05$) were also significantly higher than in the Low group (13.52 ± 3.15 ng/ml, $P < 0.001$).

4. Discussion

Our results demonstrate significant alterations in the ultrastructure of placental syncytiotrophoblasts and the mitochondrial morphology of epithelial cells in fetal capillaries following exposure to elevated concentrations of $PM_{2.5}$. These observations may indicate the possible involvement of oxidative stress, which could be induced by $PM_{2.5}$ exposure, as supported by the increased levels of MDA and SOD2. It is important to note that the ultrastructural changes observed in the High groups, as well as the elevated levels of MDA and SOD2, highlight a potential link to oxidative stress. To the best of our knowledge, this is the first study to examine the effects of particulate matter on the ultrastructure of the human placenta and mitochondria within the fetal capillaries.

The syncytiotrophoblast, a post-mitotic cell layer composed exclusively of fetal cells, is in direct contact with the maternal circulation and serves as a barrier between the mother and fetus [17]. The microvilli, which cover the contour of the syncytiotrophoblast densely, expand the connecting area to the maternal intervillous space from five- to seven-fold more [25]. The reduction in the microvillus surface, due to its shortening, indicates a decrease in the exchange rate of nutrients, oxygen, and waste. The expanded basement membrane has also been demonstrated to interfere with the efficiency of nutrient and gas exchange from mother to fetus [26]. As demonstrated by previous research, the placenta from early pregnancy failure exhibits microvilli loss with ER stress [14]. The thickening or detachment of the basement membrane in the placenta, as reported in cases of IUGR in the presence of inflammatory lesions or hypoxic conditions, are consistent with the findings of this present study [15,27–29]. According to previous studies, the deposition of $PM_{2.5}$ leads to elevated inflammation and ER stress [30]. Vacuolization, an indicator of cell death, is observed in the deteriorated syncytiotrophoblasts exposed to high oxygen levels [31]. These previous study results including shortening of microvilli, vacuolization, ER swelling in syncytiotrophoblast area, and basement membrane thickening are consistent with our current microscopic observations.

Mitochondria are key sites for the generation of ROS to synthesize ATP via oxidative phosphorylation and are sensitive to ROS-mediated damage [7]. Pregnancy itself is a factor that increases oxidative stress [32,33], and can produce ROS in the ER, cell membranes, and mitochondria [34]. Mitochondria isolated from preeclampsia and GDM patients show increased apoptotic protein concentrations with swelling of the membrane and cristae [35,36]. Alteration in mitochondrial morphology has been recognized as a functional change with increased expression of P450scc, an enzyme that converts cholesterol to pregnenolone [37]. The focus of this study was mitochondria present in the endothelial cells of fetal capillaries, because the mitochondrial

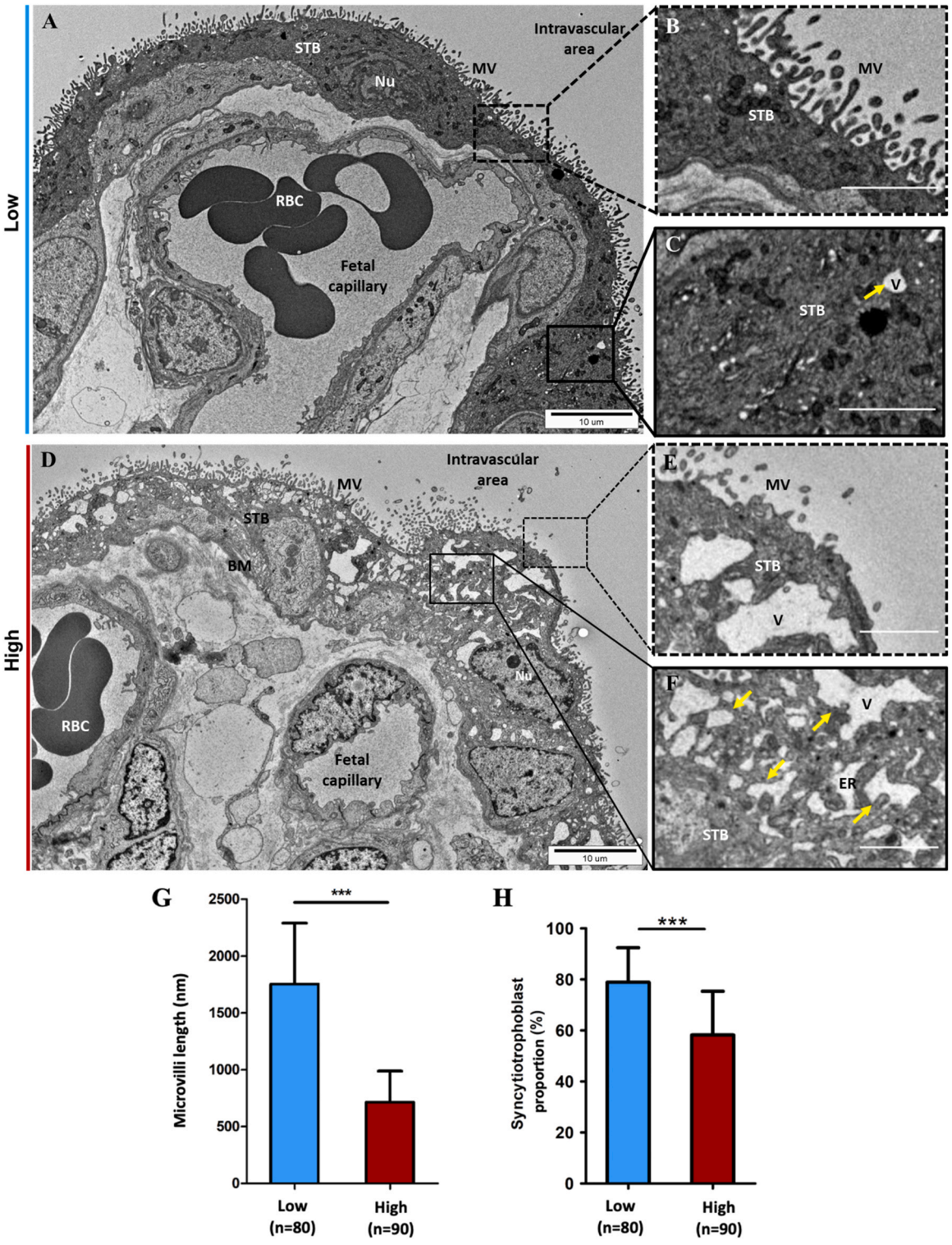


Fig. 1. TEM images of *p*lacental tissue from the low group (A-C) and the high group (D-F). as shown in *p*anels A–F, ultrastructural differences in microvilli morphology and vacuole formation (yellow arrows) within the syncytiotrophoblast. quantitative analyses of microvilli length (G) and syncytiotrophoblast tissue *p*roportion (H) are shown as mean ± SD with significant difference. Abbreviations: BM, basement membrane; ER, endoplasmic reticulum; M, mitochondria; MV, microvilli; Nu, nucleus; RBC, red blood cell; STB, syncytiotrophoblast; V, vacuole. Scale bars: 10μm (A, D); 1μm (B, C, E, F). $^{***}p < 0.001$.

structures in syncytiotrophoblasts are irregular and atypical in shape [38]. In our study, double membrane swelling and cristae damage of mitochondria in fetal blood vessels were more prevalent in the High $PM_{2.5}$ group compared to the Low $PM_{2.5}$ group. However, the mechanisms underlying the effects of $PM_{2.5}$ on mitochondrial dynamics, including double membrane disruption and cristae rupture, remain unclear.

The end product of membrane lipid peroxidation, MDA, which is produced when polyunsaturated fatty acids are peroxidized, has been used as a ROS biomarker [39]. The levels of MDA were significantly higher in the High group compared to the Low group in our results. To maintain a balanced physiological level of ROS, antioxidants are

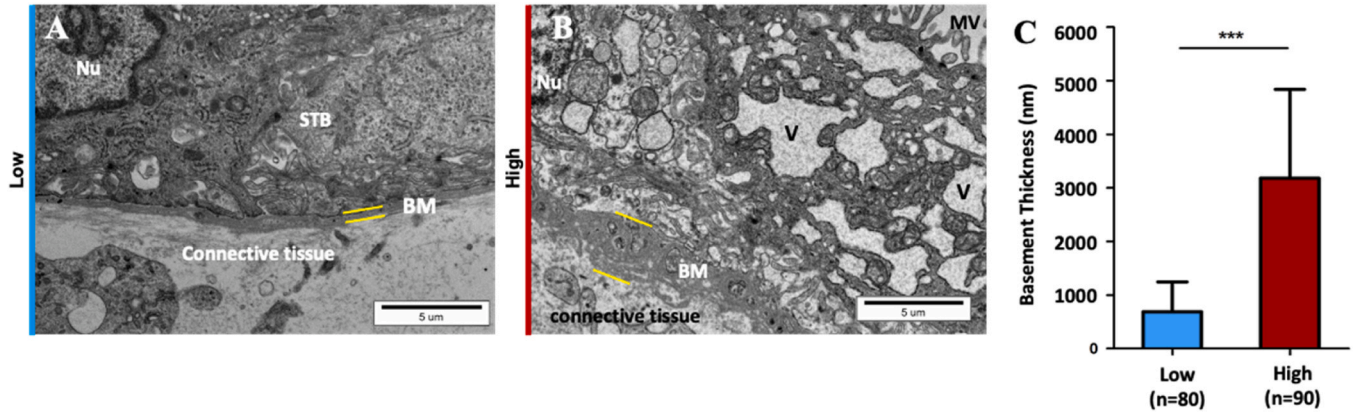


Fig. 2. Comparison of syncytiotrophoblast-side basement membrane thickness between the low (A) and the high (B) groups. The measured basement membrane thickness values are shown in a bar graph (C) as mean ± SD. Yellow bars in (A) and (B) indicate the thickness of the basement membrane, respectively. Abbreviations: BM, basement membrane; MV, microvilli; Nu, nucleus; STB, syncytiotrophoblast; V, vacuole. Scale bar: 5μm (A, B). $^{***}p < 0.001$.

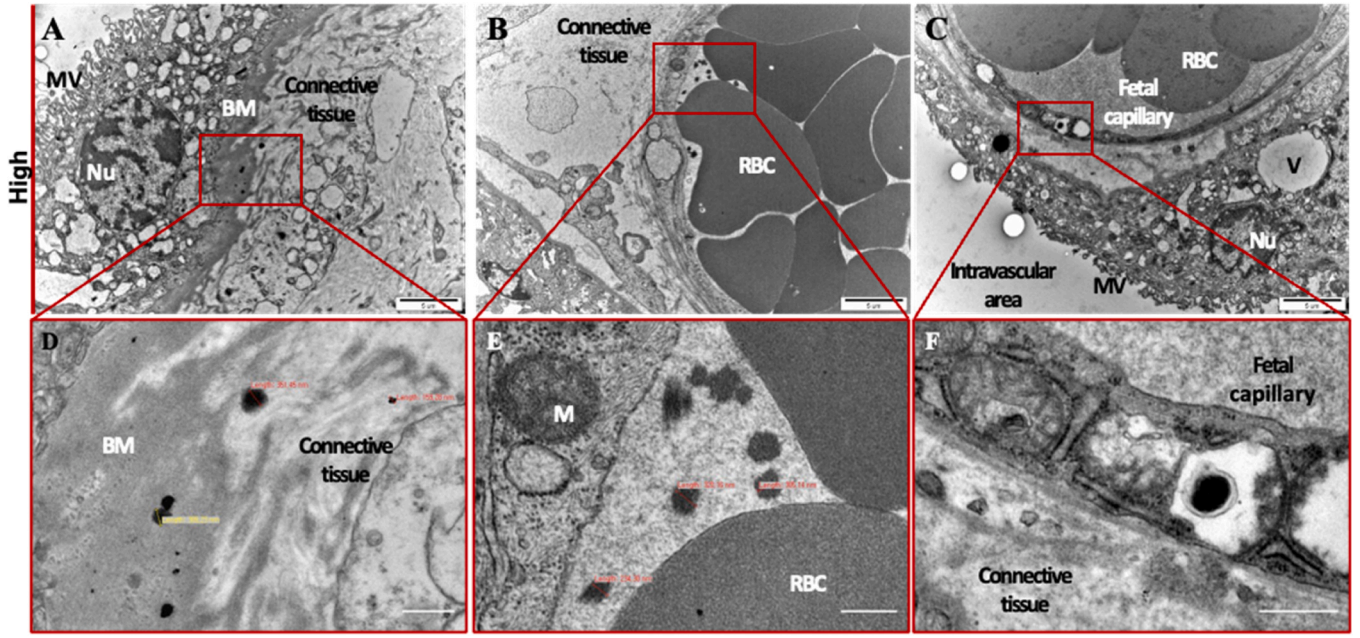


Fig. 3. Presence of unidentified nano-size particles in the high group placenta. Unspecified nano-size substances were observed not only under the basement membrane (A, D), but also inside of fetal capillary (B, E) and fetal blood vessel (C, F) in the high group placenta. Encapsulated black particle is observed in the epithelial cell of fetal capillary (C, F). abbreviations: BM, basement membrane; M, mitochondria; MV, microvilli; Nu, nuclear; RBC, red blood cell; STB, syncytiotrophoblast; V, vacuole. Scale bar: 5μm (A – C); 1μm (D – F).

produced in response to reduce ROS [40]. The antioxidant SOD2 has been identified as a biomarker of PTB in the amniotic fluid and a prognostic indicator of gestational age [41]. Our results also showed significantly higher levels of SOD2 in placental tissue with high $PM_{2.5}$. Therefore, in accordance with our previous study of mitochondrial OXPHOS dysfunction induced by $PM_{2.5}$ in cord blood [10], these present findings suggest that the comprehensive observation of mitochondrial structural change and the upregulation of MDA and SOD2 in placenta tissue may be associated with $PM_{2.5}$ exposure. Given that both $PM_{2.5}$ and oxidative stress have been implicated in the modulation of mitochondrial dynamics [42,43], further investigations are required to elucidate the precise mechanisms through which $PM_{2.5}$ may contribute to mitochondrial alterations.

While the observations suggest the oxidative stress, which could be induced by $PM_{2.5}$ exposure, as indicated by the increased levels of MDA and SOD2, this study has a few limitations. Firstly, because the sample size was relatively small, various delivery types and pregnancy complications such as PTB, GDM, and SGA were included in the Low group. These complications may influence birth weight and structural changes. However, in our previous studies, which were conducted with a large sample size using adjusted multivariable models, the High group exhibited a significantly lower birth weight [4,10,44]. Delivery type – normal delivery and cesarean section – can be major factors influencing the placental structure. However, the analysis of the cesarean section sample alone showed significant alterations in shortening of microvilli length, proportion of syncytiotrophoblast tissue induced by vacuolization and ER swelling, basement thickness, and structural change of mitochondria in fetal blood vessels ($P < 0.05$). Second, while we observed the presence of nano-sized particles in the placental tissue of the High group, we were not able to conduct compositional analyses such as energy-dispersive X-ray spectroscopy (EDS) or spectrometry to confirm their elemental composition. As such, these findings are reported as observational, indicating a potential possibility of an association with PM exposure, though no direct causal inference can be drawn.

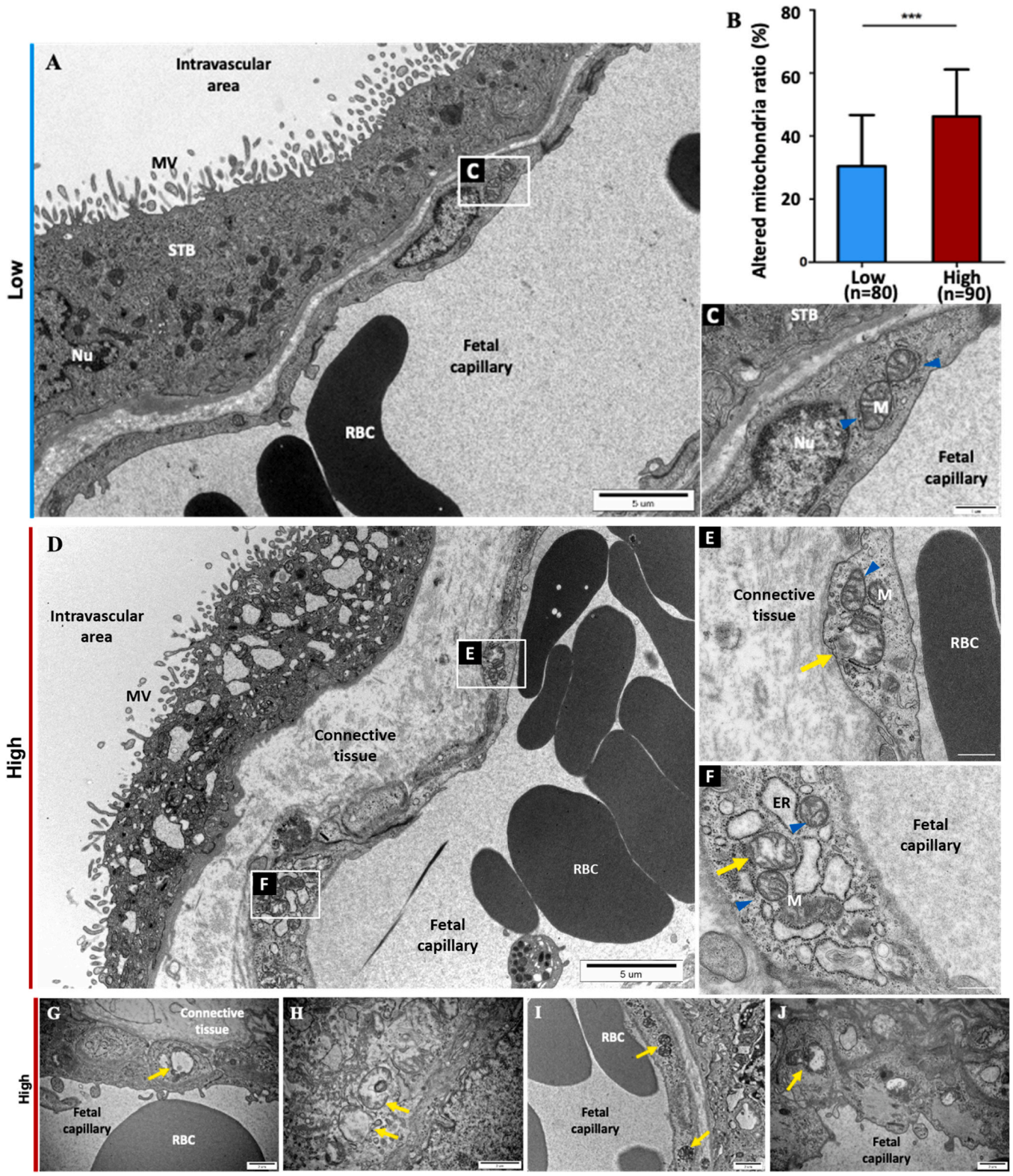


Fig. 4. Mitochondrial alterations in the endothelial cells of the fetal capillaries from the low (A, C) and the high (D–J) groups. The alteration of mitochondria structure ratio in the epithelial cells of the fetal capillaries (B). blue arrow heads indicate normal mitochondria, and the yellow arrows indicate structural alteration of mitochondria. Abbreviations: BM, basement membrane; M, mitochondria; MV, microvilli, Nu, nuclear; RBC, red blood cell; STB, syncytiotrophoblast; V, vacuole. Scale bar: 5μm (A, D); 2μm (G − F); 1μm (B, C, and E). ***: $p < 0.001$.

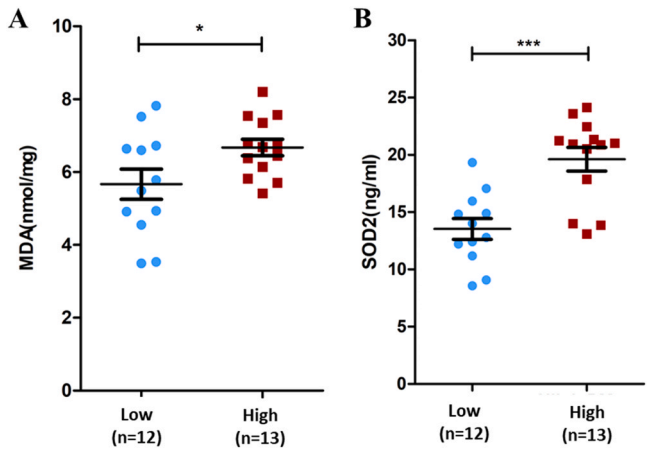


Fig. 5. Increased levels of SOD2 and MDA expression in the *p*lacenta with the elevated $pM_{2.5}$. MDA (A) and SOD2 (B) levels were analyzed with ELISA from the low group (n = 12) and the high group (n = 13). samples include all samples from the TEM analysis dataset and additional APPO samples. Scatter *p*lot displays individual sample values with group means ± SD indicated*: $p < 0.05$, ***: $p < 0.001$.

To improve the accuracy of understanding the effects of $PM_{2.5}$ on the placenta, it may be necessary to consider the assessment of nano-sized substances employing a more substantial sample size.

In conclusion, our findings indicate that placental ultrastructural changes are observed in association with elevated concentrations of $PM_{2.5}$. Furthermore, the increased levels of MDA and SOD2 suggest the potential involvement of oxidative stress in these mitochondrial alterations. This study suggests a possible association between prenatal exposure to $PM_{2.5}$, oxidative stress, and placental mitochondrial alterations. Further investigation is necessary to elucidate the underlying mechanism.

CRediT authorship contribution statement

Gain Lee: Writing – original draft, Visualization, Methodology, Investigation. **Jung Mi Han:** Visualization, Validation, Methodology. **Young-Ah You:** Methodology, Conceptualization. **Soo Min Kim:** Resources, Formal analysis. **Ki-Hwan Han:** Validation. **Kim Young ju:** Writing – review & editing, Supervision, Funding acquisition, Conceptualization. **Yoon-Young Go:** Writing – review & editing. **Sunwha Park:** Resources, Conceptualization. **Young Min Hur:** Resources, Investigation.

Consent to participate

All the participants provided written informed consent prior to enrolment.

Consent to publish

All authors declare their consent to publish this article.

Ethics approval

This study was approved by the Ethical Research Committees of the six centers (Ewha Womans University Mokdong Hospital, EUMC 2021–04–032) and conducted according to the ethical principles of the Helsinki Declaration.

Funding

This study was supported by the National Institute of Health Research Project (project No. 2021-ER1208-02), a grant of the Korea Health Technology R&D Project through the Korea Health Industry Development Institute (KHIDI), funded by the Ministry of Health & Welfare (RS-2023-00266554), and supported by the BK21 FOUR (Fostering Outstanding Universities for Research) funded by the Ministry of Education (MOE, Korea) and National Research Foundation of Korea (NRF-5199990614253, Education Research Center for 4IR-Based Health Care). The work was supported by the Ewha Womans University Research Grant of 2024.

Declaration of Competing Interest

The authors declare that they have no known competing financial interests or personal relationships that could have appeared to influence the work reported in this paper.

Appendix A. Supporting information

Supplementary data associated with this article can be found in the online version at doi:10.1016/j.reprotox.2025.108973.

References

[1] L. Wang, D. Luo, X. Liu, J. Zhu, F. Wang, B. Li, L. Li, Effects of PM2.5 exposure on reproductive system and its mechanisms, Chemosphere 264 (2021) 128436.
[2] K.-H. Kim, E. Kabir, S. Kabir, A review on the human health impact of airborne particulate matter, Environ. Int. 74 (2015) 136–143.
[3] I. Kloog, B. Ridgway, P. Koutrakis, B.A. Coull, J.D. Schwartz, Long-and short-term exposure to PM2. 5 and mortality: using novel exposure models, Epidemiology 24 (4) (2013) 555–561.
[4] T.G. Ahn, Y.J. Kim, G. Lee, Y.A. You, S.M. Kim, R. Chae, Y.M. Hur, M.H. Park, J. G. Bae, S.J. Lee, Y.H. Kim, S. Na, Association between individual air pollution (PM (10), PM(2.5)) exposure and adverse pregnancy outcomes in korea: a multicenter prospective cohort, air pollution on pregnancy outcome (APPO) study, J. Korean Med. Sci. 39 (13) (2024) e131.
[5] J. Park, E.H. Park, J.J. Schauer, S.-M. Yi, J. Heo, Reactive oxygen species (ROS) activity of ambient fine particles (PM2. 5) measured in Seoul, korea, Environ. Int. 117 (2018) 276–283.
[6] H. Bové, E. Bongaerts, E. Slenders, E.M. Bijnens, N.D. Saenen, W. Gyselaers, P. Van Eyken, M. Plusquin, M.B.J. Roeffaers, M. Ameloot, T.S. Nawrot, Ambient black carbon particles reach the fetal side of human placenta, Nat. Commun. 10 (1) (2019) 3866.
[7] O. Holland, M.D. Nitert, L.A. Gallo, M. Vejzovic, J.J. Fisher, A.V. Perkins, Placental mitochondrial function and structure in gestational disorders, Placenta 54 (2017) 2–9.
[8] R. Ning, Y. Shi, J. Jiang, S. Liang, Q. Xu, J. Duan, Z. Sun, Mitochondrial dysfunction drives persistent vascular fibrosis in rats after short-term exposure of PM2. 5, Sci. Total Environ. 733 (2020) 139135.
[9] J. Liu, S. Liang, Z. Du, J. Zhang, B. Sun, T. Zhao, X. Yang, Y. Shi, J. Duan, Z. Sun, PM2.5 aggravates the lipid accumulation, mitochondrial damage and apoptosis in macrophage foam cells, Environ. Pollut. 249 (2019) 482–490.
[10] Y.-A. You, S. Park, E. Kwon, Y.-A. Kim, Y.M. Hur, G.I. Lee, S.M. Kim, J.M. Song, M. S. Kim, Y.J. Kim, Maternal PM2. 5 exposure is associated with preterm birth and gestational diabetes mellitus, and mitochondrial OXPHOS dysfunction in cord blood, Environ. Sci. Pollut. Res. 31 (7) (2024) 10565–10578.
[11] M.Y. Turco, A. Moffett, Development of the human placenta, Development 146 (22) (2019).
[12] G.J. Burton, A.L. Fowden, The placenta: a multifaceted, transient organ, Philos. Trans. R. Soc. B Biol. Sci. 370 (1663) (2015) 20140066.
[13] M.A. Costa, The endocrine function of human placenta: an overview, Reprod. Biomed. Online 32 (1) (2016) 14–43.
[14] J. Hempstock, E. Jauniaux, N. Greenwold, G.J. Burton, The contribution of placental oxidative stress to early pregnancy failure, Hum. Pathol. 34 (12) (2003) 1265–1275.
[15] E.C. Castro, M.A. Reis, V.P. Teixeira, Thickening of the amnion basement membrane and its relationship to placental inflammatory lesions and fetal and maternal disorders, Eur. J. Obstet. Gynecol. Reprod. Biol. 114 (2) (2004) 171–176.
[16] N. Bachmaier, K. Linnemann, K. May, R. Warzok, S. Kuno, M. Niemeyer, S. Balk, C. Fusch, Ultrastructure of human placental tissue after 6h of normoxic and hypoxic dual in vitro placental perfusion, Placenta 28 (8-9) (2007) 861–867.
[17] I. Carrasco-Wong, M. Aguilera-Olguín, R. Escalona-Rivano, D.I. Chiarello, L. J. Barragán-Zúñiga, M. Sosa-Macías, C. Galaviz-Hernandez, S. San Martín, J. Gutiérrez, Syncytiotrophoblast stress in early onset preeclampsia: the issues perpetuating the syndrome, Placenta 113 (2021) 57–66.
[18] L.H. Oliveira, C.C. Xavier, A. Lana, Changes in placental morphology of small for gestational age newborns, J. Pedia Rio J. 78 (5) (2002) 397–402.
[19] J.C. Behlen, C.H. Lau, Y. Li, P. Dhagat, J.A. Stanley, A. Rodrigues Hoffman, M. C. Golding, R. Zhang, N.M. Johnson, Gestational exposure to ultrafine particles

reveals sex-and dose-specific changes in offspring birth outcomes, placental morphology, and gene networks, Toxicol. Sci. 184 (2) (2021) 204–213.
[20] J. Liu, L. Ren, J. Wei, J. Zhang, Y. Zhu, X. Li, L. Jing, J. Duan, X. Zhou, Z. Sun, Fine particle matter disrupts the blood–testis barrier by activating TGF-β3/p38 MAPK pathway and decreasing testosterone secretion in rat, Environ. Toxicol. 33 (7) (2018) 711–719.
[21] Y.M. Hur, S. Park, E. Kwon, Y.A. You, A. Ansari, S.M. Kim, G. Lee, M.H. Park, K. A. Lee, S.J. Kim, Y.H. Kim, Y.S. Jung, G.J. Cho, M.J. Oh, S.H. Na, S.J. Lee, T.G. An, J.G. Bae, Y.H. Kim, S.J. Lee, N.K. Kim, E.H. Ha, Y.J. Kim, The introduction to air pollution on pregnancy outcome (APPO) study: a multicenter cohort study, Obstet. Gynecol. Sci. 66 (3) (2023) 169–180.
[22] Y. Jeong, S. Park, E. Kwon, Y.M. Hur, Y.-A. You, S.M. Kim, G. Lee, K.A. Lee, S. J. Kim, G.J. Cho, M.-J. Oh, S.H. Na, Sj Lee, J.-G. Bae, Y.-H. Kim, S.-J. Lee, Y.-H. Kim, Y.J. Kim, A.s.g. The, personal exposure of PM2.5 and metabolic syndrome markers of pregnant women in South Korea: APPO study, Environ. Sci. Pollut. Res. 30 (59) (2023) 123893–123906.
[23] T.W. Kirchstetter, T. Novakov, Controlled generation of black carbon particles from a diffusion flame and applications in evaluating black carbon measurement methods, Atmos. Environ. 41 (9) (2007) 1874–1888.
[24] WorldHealthOrganization, W.H.O. Global Air Quality Guidelines: Particulate Matter (PM2.5 and PM10), Ozone, Nitrogen Dioxide, Sulfur Dioxide and Carbon Monoxide. Geneva, Switzerland, 2021.
[25] F. Teasdale, G. Jean-Jacques, Morphometric evaluation of the microvillous surface enlargement factor in the human placenta from mid-gestation to term, Placenta 6 (5) (1985) 375–381.
[26] G.J. Burton, A.L. Fowden, Review: the placenta and developmental programming: balancing fetal nutrient demands with maternal resource allocation, Placenta 33 (2012) S23–S27.
[27] M. Battistelli, S. Burattini, F. Pomini, M. Scavo, A. Caruso, E. Falcieri, Ultrastructural study on human placenta from intrauterine growth retardation cases, Microsc. Res. Tech. 65 (3) (2004) 150–158.
[28] H. Soma, T. Hata, T. Oguro, K. Fujita, M. Kudo, U. Vaidya, Characteristics of histopathological and ultrastructural features of placental villi in pregnant Nepalese women, Med. Mol. Morphol. 38 (2005) 92–103.
[29] E.A. Mahmoud, N.A. Al-Bakri, B.J. Qasim, Histopathological changes of placenta in pregnant women complicated with pregestational diabetes, J. Pharm. Sci. Res. 11 (10) (2018) 2952–2959.
[30] M. Familari, Å. Nääv, L. Erlandsson, R.U. de Iongh, C. Isaxon, B. Strandberg, T. Lundh, S.R. Hansson, E. Malmqvist, Exposure of trophoblast cells to fine particulate matter air pollution leads to growth inhibition, inflammation and ER stress, PloS One 14 (7) (2019) e0218799.
[31] S. Zhao, S. Zhong, F. Wang, H. Wang, D. Xu, G. Li, Microcystin-LR exposure decreased the fetal weight of mice by disturbance of placental development and ROS-mediated endoplasmic reticulum stress in the placenta, Environ. Pollut. 256 (2020) 113362.
[32] T. Peter Stein, T.O. Scholl, M.D. Schluter, M.J. Leskiw, X. Chen, B.W. Spur, A. Rodriguez, Oxidative stress early in pregnancy and pregnancy outcome, Free Radic. Res. 42 (10) (2008) 841–848.
[33] J.J. Fisher, L.A. Bartho, A.V. Perkins, O.J. Holland, Placental mitochondria and reactive oxygen species in the physiology and pathophysiology of pregnancy, Clin. Exp. Pharmacol. Physiol. 47 (1) (2020) 176–184.
[34] H. Sies, C. Berndt, D.P. Jones, Oxidative stress, Annu. Rev. Biochem. 86 (1) (2017) 715–748.
[35] Z. Shi, W. Long, C. Zhao, X. Guo, R. Shen, H. Ding, Comparative proteomics analysis suggests that placental mitochondria are involved in the development of pre-eclampsia, PloS One 8 (5) (2013) e64351.
[36] Q. Meng, L. Shao, X. Luo, Y. Mu, W. Xu, C. Gao, L. Gao, J. Liu, Y. Cui, Ultrastructure of placenta of gravidas with gestational diabetes mellitus, Obstet. Gynecol. Int. 2015 (1) (2015) 283124.
[37] F. Martínez, M. Kiriakidou, J.F. Strauss III, Structural and functional changes in mitochondria associated with trophoblast differentiation: methods to isolate enriched preparations of syncytiotrophoblast mitochondria, Endocrinology 138 (5) (1997) 2172–2183.
[38] D. De los Rios Castillo, M. Zarco-Zavala, S. Olvera-Sanchez, J.P. Pardo, O. Juarez, F. Martinez, G. Mendoza-Hernandez, J.J. García-Trejo, O. Flores-Herrera, Atypical cristae morphology of human syncytiotrophoblast mitochondria: role for complex v, J. Biol. Chem. 286 (27) (2011) 23911–23919.
[39] E. Niki, Lipid peroxidation products as oxidative stress biomarkers, Biofactors 34 (2) (2008) 171–180.
[40] M.H. Schoots, S.J. Gordijn, S.A. Scherjon, H. van Goor, J.-L. Hillebrands, Oxidative stress in placental pathology, Placenta 69 (2018) 153–161.
[41] T.-Y. Hsu, H.-H. Cheng, K.-C. Lan, H.-N. Hung, Y.-J. Lai, C.-C. Tsai, W.-L. Fan, S.-C. Li, The abundances of LTF and SOD2 in amniotic fluid are potential biomarkers of gestational age and preterm birth, Sci. Rep. 13 (1) (2023) 4903.
[42] A.J. Kowaltowski, A.E. Vercesi, Mitochondrial damage induced by conditions of oxidative stress, Free Radic. Biol. Med. 26 (3-4) (1999) 463–471.
[43] N. Li, C. Sioutas, A. Cho, D. Schmitz, C. Misra, J. Sempf, M. Wang, T. Oberley, J. Froines, A. Nel, Ultrafine particulate pollutants induce oxidative stress and mitochondrial damage, Environ. Health Perspect. 111 (4) (2003) 455–460.
[44] S. Park, E. Kwon, G. Lee, Y.-A. You, S.M. Kim, Y.M. Hur, S. Jung, Y. Jee, M.H. Park, S.H. Na, Y.-H. Kim, G.J. Cho, J.-G. Bae, S.-J. Lee, S.H. Lee, Y.J. Kim, Correction: park et al. Effect of particulate matter 2.5 on fetal growth in Male and preterm infants through oxidative stress, Antioxidants 2023 12 (2) (2024) 135.